Phys. Lett. B 868 (2025) 139637

Contents lists available at ScienceDirect

Physics Letters B

journal homepage: www.elsevier.com/locate/physletb

Letter

Calculation of the axial-vector coupling constant g_A to two loops in covariant chiral perturbation theory

Véronique Bernard [a], Jambul Gegelia [b,c], Shayan Ghosh [d], Ulf-G. Meißner [d,e,f,*]

[a] Université Paris-Saclay, CNRS/IN2P3, IJCLab, 91405 Orsay, France
[b] Ruhr-Universität Bochum, Fakultät für Physik und Astronomie, Institut für Theoretische Physik II, D-44780 Bochum, Germany
[c] Tbilisi State University, 0186 Tbilisi, Georgia
[d] Helmholtz-Institut für Strahlen- und Kernphysik and Bethe Center for Theoretical Physics, Universität Bonn, D-53115 Bonn, Germany
[e] Institute for Advanced Simulation (IAS-4), Forschungszentrum Jülich, D-52425 Jülich, Germany
[f] Peng Huanwu Collaborative Center for Reserch and Education, International Institute for Interdisciplinary and Frontiers, Beihang University, Beijing 100191, China

ARTICLE INFO

Editor: A. Schwenk

ABSTRACT

We present a calculation of the leading two-loop corrections to the axial-vector coupling constant g_A in two covariant versions of two-flavor baryon chiral perturbation theory. Taking the low-energy constants from a combined analysis of elastic and inelastic pion-nucleon scattering, we find that these corrections are rather moderate.

1. Introduction

The nucleon axial-vector coupling constant g_A plays an eminent role in neutron β-decay, see Ref. [1] for a recent work, in nuclear reactions and in neutrino scattering off nuclei, as witnessed by the T2K, NOvA, MINERvA, MicroBooNE, and SBN experiments. For reviews, see Refs. [2,3]. Furthermore, g_A is a fundamental parameter of low-energy chiral QCD dynamics which parameterizes the leading order pion-nucleon interaction as at tree level the Goldberger-Treiman relation (GTR) allows to express the pion-nucleon coupling in terms of the axial-vector coupling. Corrections to the GTR are known to be small so that this relation is an approximate one when considering loops. The axial-vector coupling is also considered a "gold-plated" observable for the *ab initio* lattice QCD approach. The first high-precision lattice QCD calculation was reported in Ref. [4] and a summary of older and more recent results is collected in Ref. [5]. Most of these simulations are performed for unphysical pion masses, while in Refs. [6–9] the physical pion mass is also considered. In any case, the issue of precise and controlled chiral extrapolations is still of relevance. Of course, it is also of general interest to study the higher-order corrections in the quark mass expansion of this observable, as they encode information about the convergence of two-flavor baryon chiral perturbation theory. Therefore, in this work, we consider the calculation of g_A to two loops using two different covariant schemes, namely the extended-on-mass-shell (EOMS) approach [10] and the method of infrared regularization (IR) [11]. Detailed discussions of these schemes and comparisons with the often used heavy baryon approach can be found in Refs. [12,13]. This work differs from the earlier paper [14], where renormalization group methods were applied to the chiral pion-nucleon Lagrangian in the heavy baryon approach and the two-loop representation was confronted with then existing lattice calculations at unphysical pion masses. We will come back to that work later.

This article is organized as follows. In Sec. 2 we present the general form of the chiral expansion of g_A. Sect. 3 outlines the calculations of the two-loop corrections. We present and discuss our results in Sec. 4. Appendix A contains some further results.

2. Chiral expansion of g_A

In baryon chiral perturbation theory (BCHPT), one encounters odd and even powers of the small expansion parameter q, which in the two flavor case is given by pion masses and momenta as well as nucleon three-momenta. The nucleon mass m_N is of the same size as the hard scale related to chiral symmetry breaking, often estimated as $\Lambda_\chi = 4\pi F_\pi \simeq 1.2$ GeV, with $F_\pi \simeq 92$ MeV the pion decay constant. Tree diagrams start contributing at

* Corresponding author.
E-mail address: meissner@hiskp.uni-bonn.de (U.-G. Meißner).

https://doi.org/10.1016/j.physletb.2025.139637
Received 16 May 2025; Received in revised form 2 June 2025; Accepted 3 June 2025
Available online 6 June 2025

order q, one-loop diagrams at order q^3, two-loop ones at order q^5, three-loop diagrams at order q^7, and so on. In this paper we will concentrate on the leading two-loop diagrams of chiral order q^5, the order q^6 two-loop calculation is in progress [20]. The latter involves the calculation of several two-loop diagrams with vertices from $\mathcal{L}_{\pi N}^{(2)}$. Consequently, the chiral expansion of the axial-vector coupling as evaluated in this work takes the form

$$\begin{aligned} g_A &= g_0 \left\{ 1 + \left(\frac{\alpha_2}{(4\pi F)^2} \ln\frac{M}{\mu} + \beta_2 \right) M^2 + \alpha_3 M^3 \right. \\ &\quad \left. + \left(\frac{\alpha_4}{(4\pi F)^4} \ln^2\frac{M}{\mu} + \frac{\gamma_4}{(4\pi F)^4} \ln\frac{M}{\mu} + \beta_4 \right) M^4 \right\} + \mathcal{O}(M^5) , \\ &= g_0 \left\{ 1 + \underbrace{\Delta^{(2)} + \Delta^{(3)}}_{\text{one-loop}} + \underbrace{\Delta^{(4)}}_{\text{leading two-loop}} \right\} + \mathcal{O}(M^5) , \end{aligned} \tag{1}$$

with g_0 the chiral limit value of g_A,

$$g_A = g_0 \left[1 + \mathcal{O}(M^2) \right] , \tag{2}$$

and $\Delta^{(4)}$ contains the two loop contribution of chiral order q^5, as well as contributions from one loop diagrams with vertices from $\mathcal{L}_{\pi N}^{(1,2,3)}$. Note that terms with denominations one-loop/leading two-loop in the last line of Eq. (1) include the contributions from tree diagrams with vertices from $\mathcal{L}_{\pi N}^{(3/5)}$. Further, μ is the scale of dimensional regularization and $\Delta^{(n)}$ represents the correction at order n in the chiral counting. We have expressed g_A in terms of the pion decay constant in the chiral limit, F, and the leading order term of the quark mass expansion of the pion mass squared, M^2. One has:

$$F_\pi = F \left[1 + \mathcal{O}(M^2) \right] , \quad M_\pi^2 = M^2 \left[1 + \mathcal{O}(M^2) \right] . \tag{3}$$

The difference between F and F_π (M and M_π) is of higher order when working at $\mathcal{O}(q^3)$, however, at the order we are working it has to be taken into account. The one-loop coefficients α_2 and β_2 in Eq. (1) were first given in Ref. [15] and the one-loop fourth order calculation was completed in Ref. [16] with (see also Ref. [17]),

$$\begin{aligned} \alpha_2 &= -2 - 4g_0^2 , \\ \beta_2 &= \frac{4}{g_0} d_{16}^r(\mu) - \frac{g_0^2}{(4\pi F)^2} , \\ \alpha_3 &= \frac{1}{24\pi F^2 m} \left(3 + 3g_0^2 - 4mc_3 + 8mc_4 \right) , \end{aligned} \tag{4}$$

with m the nucleon mass in the two-flavor chiral limit (sometimes also denoted as m_0). Further, the expressions in Eq. (4) are identical in the IR and EOMS schemes when expanded in powers of M. Indeed in the latter the additional so-called regular terms, which violate the power counting, can be absorbed into the LECs g_0 and d_{16}, see Ref. [18] and below. One has in the EOMS scheme

$$g_0 \to g_0 + \delta g_0|_{\text{reg}} \quad d_{16} \to d_{16} + \delta d_{16}|_{\text{reg}} , \tag{5}$$

where the subscript "reg" denotes the above mentioned regular terms.

Let us now discuss the M^4 contribution to g_A. Note that contrary to the work [14], in which α_4 was calculated in heavy baryon chiral perturbation theory using renormalization group methods, we use here the operator basis and low-energy constants (LECs) given in Ref. [19]. There are four types of contributions to $\Delta^{(4)}$: the irreducible diagrams, the one coming from the wave function and coupling constant renormalization, the one loop graphs with vertices from $\mathcal{L}_{\pi N}^{(3)}$, and counterterms. One thus has schematically

$$g_0\, \Delta^{(4)} = g_A^{\text{ren}} + g_A^{d_i} + g_A^{\text{irr}} + g_A^{\text{ct}} . \tag{6}$$

3. Outline of the calculation

Here, we sketch the calculation of the four different contributions mentioned above. For all the details, we refer to Ref. [20].

Let us first discuss the wave function and coupling constant renormalization. The wave function renormalization constant Z is the residue of the pole in the two point function and is determined by

$$Z^{-1} = 1 - \frac{d}{d\not p} \Sigma(\not p) \bigg|_{\not p = m_N} \tag{7}$$

with $\Sigma(\not p)$ the nucleon self-energy, which has a similar expansion as discussed above for g_A, namely

$$Z = 1 + Z_{1-\text{loop}} + Z_{2-\text{loop}} + \cdots , \tag{8}$$

where one has

$$\begin{aligned} Z_{1-\text{loop}} &= -\frac{9}{32\pi^2 F^2} M^2 g_0^2 \left\{ 16\pi^2 \lambda + \log\frac{M}{\mu} + \frac{1}{3} - \frac{\pi M}{2m} - \epsilon \left[\log^2\frac{M}{\mu} + \frac{2}{3} \log\frac{M}{\mu} \right. \right. \\ &\qquad \left. \left. + \frac{1}{24}(6 + \pi^2) - \frac{\pi}{m} M \left(\log\frac{M}{\mu} - \frac{1}{6}(1 + 6\log 2) \right) \right] \right\} \\ &\quad + \frac{3}{16\pi^2 F^2} M^2 g_0^2 \left\{ 16\pi^2 \lambda + \log\frac{m}{\mu} - \frac{1}{2} - \epsilon \left[\log^2\frac{m}{\mu} - \log\frac{m}{\mu} + \frac{1}{4}\left(5 + \frac{\pi^2}{6} \right) \right] \right\} \end{aligned} \tag{9}$$

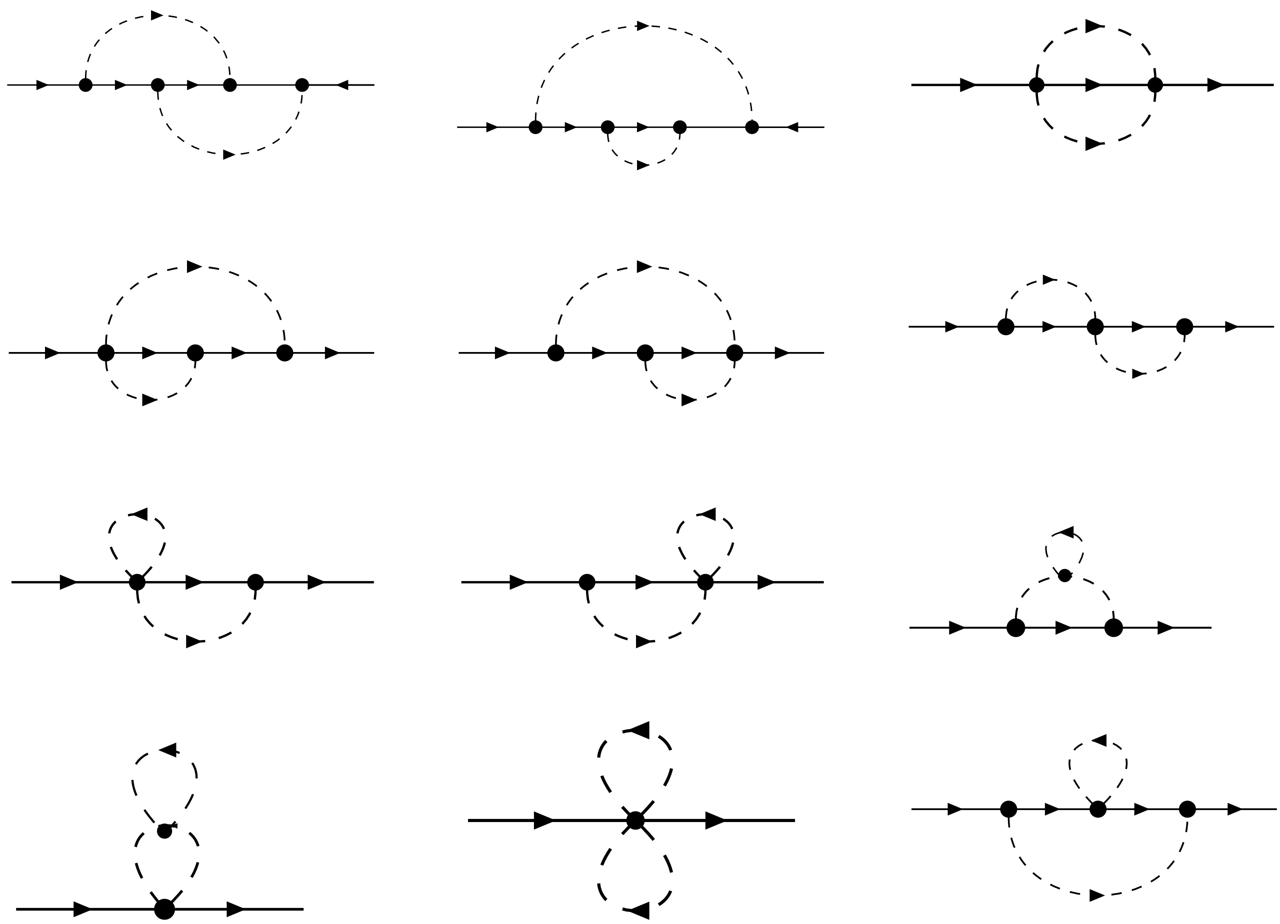

Fig. 1. Two-loop diagrams contributing to the nucleon self-energy. The same topologies contribute also to g_A. For the latter one has to hook the axial current wherever possible on the nucleon propagator and on the vertices with pions and nucleons. The dashed lines represent the pion and the solid ones the nucleon. The dots are vertices from $\mathcal{L}^{(1)}_{\pi N}$ at the order we are working. Note that there are further two-loop diagrams shown in Fig. 2 where the axial-current couples to three pions.

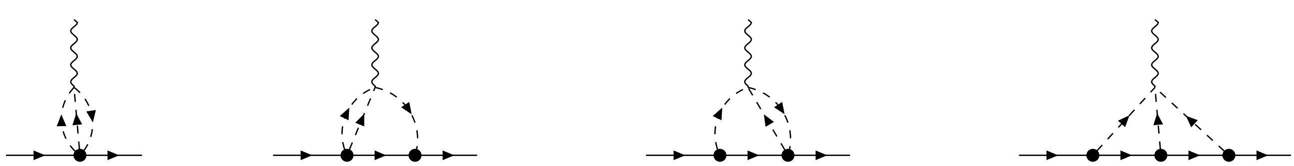

Fig. 2. Two-loop diagrams contributing to g_A. The wavy line represents the axial current, the dashed ones the pion and the solid lines the nucleon.

with

$$\lambda = \frac{1}{16\pi^2}\left(\frac{1}{d-4} - \frac{1}{2}\left(\log(4\pi) - \gamma_E + 1\right)\right) \equiv -\frac{1}{32\pi^2}\lambda_0 \,, \tag{10}$$

and γ_E is the Euler-Mascheroni constant. The first two lines correspond to the pure infrared result while the last line gives the contribution from the regular part. As expected the latter exhibits only analytic terms in M^2. The total sum given in Eq. (9) is the EOMS result expanded up to M^3. Note that one needs the results of the one-loop calculation up to order $\mathcal{O}(\epsilon)$ as it contributes to the product of two one-loop quantities. Further, $d = 4 - 2\epsilon$ is the dimension of the space-time. $Z_{2-\text{loop}}$ can be obtained from the nucleon self-energy to two loops, whose purely IR part is given in Ref. [21] and in Refs. [22–25] within the EOMS scheme. In order to calculate the Z factor we have performed the calculation of $\Sigma(p^2)$ at two loop order, see the diagrams in Fig. 1, and found agreement with these works at the order we are working. We thus finally have

$$g_A^{\text{ren}} = g_0 \left(\left(\Delta^{(2)} + \Delta^{(3)}\right) Z_{1-\text{loop}} + g_0 \left(Z^2_{1-\text{loop}} + Z_{2-\text{loop}} \right) \right) . \tag{11}$$

Let us turn to g_A^{irr}. There are 44 irreducible diagrams contributing at two loop order. Forty have the same topologies as the ones for the nucleon mass with the axial current interacting with the nucleon and up to four pions wherever possible. For example the first graph in Fig. 1 leads to 7 diagrams, the second and third ones to 8 diagrams each, and so on. They are proportional to $g_0^{1,3,5}$. Additionally there are four diagrams specific to the calculation of the axial current, where the axial current couples to three pions, see Fig. 2. In order to calculate these 44 graphs we used the Mathematica program Feyncalc [26], TARCER [27] and finally HypExp to expand the Hypergeometric functions [28]. It allows to write the result in terms of a small set of scalar master integrals $F_{\alpha\beta\gamma\delta\epsilon}(m_1, m_2, m_3, m_4, m_5)$ with two integration variables involving up to five propagators:

$$F_{\alpha\beta\gamma\delta\epsilon}(m_1,m_2,m_3,m_4,m_5) = \int \frac{d^dk}{(2\pi)^d}\frac{d^dk'}{(2\pi)^d}\frac{1}{[k^2-m_1^2]^\alpha[k'^2-m_2^2]^\beta[(k-p)^2-m_3^2]^\gamma[(k'-p)^2-m_4^2]^\delta[(k-k')^2-m_5^2]^\epsilon}, \tag{12}$$

with m_i denoting here either the nucleon or the pion mass. These functions also depend in principle on p^2, but unless specified otherwise they are understood to be taken at $p^2=m^2$ in the following. Note that when $\beta=0$ and $\gamma=0$ these functions are the well-known sunset integrals which have been rather well studied in the literature, using the Mellin-Barnes representation, see for example Ref. [29] (and references therein). In particular the full ϵ-dependent expression of the functions $F_{1,0,0,1,1}(M,m,M)$ and $F_{2,0,0,1,1}(m,M,M)$ to all orders in M is given in Ref. [30] providing some checks of our results. Following Ref. [21] we split these loop functions into a purely infrared part F_4, a mixed term F_2+F_3 and a regular part F_1:

$$F_{\alpha\beta\gamma\delta\epsilon}(m_1,m_2,m_3,m_4,m_5) = F_1+(F_2+F_3)+F_4\,. \tag{13}$$

This decomposition corresponds to an expansion of the integrand into different regions where the integration momenta is either of the order of the soft scale or of the hard scale. More precisely, in F_4 both integration momenta are soft, whereas in F_2, F_3 one of these is soft and the other hard, and in F_1 they are both hard. The latter terms can be absorbed by the LECs. This decomposition allows to differentiate between the pure IR result and the full EOMS one. At present we have performed an expansion of these loop functions up to order M^5.

For the pure IR result for g_A as well as for the two-loop contributions to Z we need four two-loop functions, namely

$$F_{1,0,0,1,1}(M,m,M),\ F_{2,0,0,1,1}(m,M,M),\ F_{1,0,1,1,1}(M,m,m,M),\ F_{1,1,1,1,1}(M,M,m,m,M)\,, \tag{14}$$

with M and m the leading order terms of the quark mass expansion of the pion and the nucleon mass, respectively. For the graphs with the axial coupling to three pions, we need three additional loop functions with three pion propagators instead of two:

$$F_{1,0,1,1,1}(m,M,M,M),\ F_{1,1,1,1,1}(M,M,m,m,M),\ F_{1,1,0,0,1}(M,M,M)|_{p^2=0}\,, \tag{15}$$

and one with two pion propagators $F_{2,0,0,1,1}(M,m,M)$, which is, however, not an independent loop function as it can be expressed in terms of $F_{1,0,0,1,1}(M,m,M)$ and $F_{2,0,0,1,1}(m,M,M)$ [31]. In the case of the second and third scalar integrals in Eq. (15) we only need the first term of the expansion in M which we take from Ref. [32]. For the EOMS calculation more loop functions are needed which involve only one pion mass, thus contributing only to $F_{1,2,3}$. These are

$$F_{1,0,0,1,1}(M,m,m)|_{p^2=0,m^2},\ \ F_{1,0,1,1,1}(M,m,m,m)\,. \tag{16}$$

Indeed those necessarily have $F_4\equiv 0$. One also needs the products of two one-loop functions

$$A(m_1) = \int \frac{d^dk}{(2\pi)^d}\frac{1}{[k^2-m_1^2]}\,,$$
$$B(m_1,m_2) = \int \frac{d^dk}{(2\pi)^d}\frac{1}{[k^2-m_1^2][(k-p)^2-m_2^2]}\,, \tag{17}$$

which are well known in one loop calculation within BCHPT.

Let us now turn to the contribution of one-loop graphs with either vertices from $\mathcal{L}^{(3)}_{\pi N}$ or insertions from mesonic operators with LECs from $\mathcal{L}^{(4)}_{\pi\pi}$. This contribution denoted as $g_A^{d_i}$ is necessary to cancel the divergences $\sim\log(M/\mu)/\epsilon$ and $\sim\log(m/\mu)/\epsilon$ appearing in the two-loop calculation. In fact this property was used in Ref. [14] to determine α_4 from a renormalization group condition. Here this cancellation provides one of the various checks of the result. The LECs of this part of the chiral pion-nucleon Lagrangian are usually denoted as d_i and nine of them contribute to g_A at $\mathcal{O}(q^4)$, namely $d_{1,2,10,11,12,13,14,16,18}$. They satisfy

$$d_i = \mu^{-2\epsilon}\left(\delta_i\lambda + d_i(\mu) + \epsilon\, d_i^\epsilon(\mu) + \mathcal{O}(\epsilon^2)\right) \tag{18}$$

with the δ_i given in Ref. [19] for the IR case and in Ref. [18] for the full EOMS case. Note that each δ_i has an expansion in powers of g_0, which up to the order we are working has the form

$$\delta_i = \delta_i^{(0)} + \delta_i^{(1)}g_0 + \delta_i^{(2)}g_0^2 + \delta_i^{(3)}g_0^3 + \delta_i^{(4)}g_0^4 + \mathcal{O}(g_0^5)\,, \tag{19}$$

where the δ_i with $i=(1,2)/(10-13,16)$ have non-vanishing contributions of only even/odd powers of g_0 respectively, while for $i=14$ only $\delta_{14}^{(4)}$ is different from zero. This has to be kept in mind when checking the scale dependence. There are also contributions from the mesonic LECs l_3 and l_4, which enter the quark mass expansion of the pion mass and the pion decay constant, respectively. Similarly to the d_i one has

$$l_i = \mu^{-2\epsilon}\left(\gamma_i\lambda + l_i(\mu) + \epsilon\, l_i^\epsilon(\mu) + \mathcal{O}(\epsilon^2)\right) \tag{20}$$

with

$$\gamma_3 = -\frac{1}{2},\ \gamma_4 = 2\,. \tag{21}$$

We have given the LECs up to order ϵ as they will be multiplied by one-loop terms and thus the ϵ terms can contribute at two-loop order. The result of a one-loop calculation can be written in terms of a sum of some scalar master integrals which can be split into an infrared part (I) and a regular one (R) with coefficients $c^n_{I,R}$. One can decompose the contributions from the insertions of the d_i as

$$g_A^{d_i} = d_i\sum_n (I^n c_I^n + R^n c_R^n) = \sum_n I^n c_I^n d_i|_{IR} + \sum_n (R^n c_R^n d_i|_{IR} + I^n c_I^n d_i|_R) + \sum_n R^n c_R^n d_i|_R\,, \tag{22}$$

where $d_i|_{IR}$ contains the δ_i from Ref. [19] and $d_i|_R$ contains the difference between the EOMS and IR results for the δ_i. The first sum in the last equality in Eq. (22) added to the IR two-loop contributions constitutes the IR result. It satisfies the Ward identities. The same is true for the second sum together with the mixed terms from the two-loop graphs, which we will call the mixed result. Finally one has the contribution from the third sum and the regular part of the two loop graphs which can be absorbed into $g_A^{\rm ct}$. The EOMS result is the sum of these three parts.

Finally, we discuss the last contribution to the two-loop calculation of g_A. In Eq. (6) $g_A^{\rm ct}$ denotes counterterms generated by a linear combination of LECs from the Lagrangian at order q^5:

$$g_A^{\rm ct} = \left(C^{(0)} + C^{(1)} g_0 + C^{(2)} g_0^2 + C^{(3)} g_0^3 + C^{(5)} g_0^5\right)\, M^4 \equiv C\, M^4\, . \tag{23}$$

They are necessary to absorb the remaining infinities, however, as explained before, they cannot cancel the $\log M/\epsilon$ terms as they are coefficients of an analytic term in the expansion of g_A. One has

$$\begin{aligned} C &= \mu^{-4\epsilon}\, \left(C_2\lambda_2 + C_1(\mu)\lambda_1 + C_0(\mu) + \mathcal{O}(\epsilon)\right)\, , \\ &= \mu^{-4\epsilon} \sum_{i=1,2,3,5} \left(C_2^{(i)} g_0^i \lambda_2 + C_1^{(i)}(\mu) g_0^i \lambda_1 + C_0^{(i)}(\mu) g_0^i + \mathcal{O}(\epsilon)\right)\, , \end{aligned} \tag{24}$$

with

$$\begin{aligned} \lambda_2 &= \lambda_0^2 + \left(\log(4\pi) - \gamma_E + 1\right)^2\, , \\ \lambda_1 &= \lambda_0 + \left(\log(4\pi) - \gamma_E + 1\right)\, , \end{aligned} \tag{25}$$

which is appropriate for the modified $\overline{\rm MS}$ subtraction scheme used here as it is customary in CHPT (for similar results in two-loop calculation in the meson sector see, e.g., Ref. [33]). Let us consider the derivative of C with respect to μ. It turns out that the contribution to g_0^i of this derivative is not given by the derivative of $C^{(i)}$ with respect to μ as the latter can contribute to various powers of g_0. This is specific to the baryon sector as already encountered in the case of the d_i, see discussion after Eq. (19). The $C^{(i)}$ therefore can not be individually scale-independent. Thus one has

$$\mu \frac{d}{d\mu} C = 0\, , \tag{26}$$

meaning of course that each contribution to g_0^i of the derivative of C with respect to μ is a scale-independent quantity. Consequently, C_2 has to be scale-independent whereas the two others are scale-dependent and satisfy the following relations [34]

$$\frac{d}{d\mu} C_1(\mu) = \frac{4C_2}{\mu}, \;\; \frac{d}{d\mu} C_0(\mu) = \frac{4C_1(\mu)}{\mu}\, . \tag{27}$$

To get these relations provides another check of the calculation together with the scale-independence of the result. One obtains

$$\begin{aligned} C^{(0)} &= \frac{8\pi^2}{F^2}\, \left(-20 d_{16}^r + 8 d_{18}^r + 14 d_{10}^r + 8 d_{11}^r + 3 d_{12}^r + d_{13}^r\right)\, \lambda_1 + C_0^{(0)}(\mu)\, , \\ C^{(1)} &= -\frac{7}{12F^4}\lambda_2 + \lambda_1 \left\{ -\frac{16\pi^2}{F^2}\left(d_{14}^r - 2(d_1^r + d_2^r)\right) - \frac{32\pi^2}{F^4}\left(l_3^r - l_4^r\right) - \frac{323}{144F^4} \right\} + C_0^{(1)}(\mu)\, , \\ C^{(2)} &= \frac{128\pi^2}{F^2}\, \left(d_{18}^r - 3 d_{16}^r\right)\, \lambda_1 + C_0^{(2)}(\mu)\, , \\ C^{(3)} &= \frac{7}{12F^4}\lambda_2 + \left\{ -\frac{64\pi^2(l_3^r - l_4^r)}{F^4} + \frac{1}{72F^4}(65 - 32\pi^2) \right\} \lambda_1 + C_0^{(3)}(\mu)\, , \\ C^{(5)} &= \frac{4}{F^4}\lambda_2 - \frac{11}{6F^4}\lambda_1 + C_0^{(5)}(\mu)\, . \end{aligned} \tag{28}$$

4. Results and discussion

We can now put all pieces together. We start with the infrared result for $Z_{(2-\text{loop})}$, which reads

$$\begin{aligned} Z_{(2-\text{loop})}|_{IR} = \frac{3M^4}{2048\pi^4 F^4} g_0 \Bigg\{ & g_0^4 \left[\frac{5\lambda_2}{4} + \lambda_1 \left(1 - 5\log\frac{M}{\mu}\right) + 10\log^2\frac{M}{\mu} - 4\log\frac{M}{\mu} + \frac{1}{24}\left(6 + 281\pi^2\right) \right] \\ & + g_0^2 \left[-3\lambda_2 + \lambda_1 \left(12\log\frac{M}{\mu} + 5\right) - 24\log^2\frac{M}{\mu} - 20\log\frac{M}{\mu} - \frac{\pi^2}{2} - 5 \right] \\ & + \left[\frac{3\lambda_2}{2} + \lambda_1 \left(2 - 6\log\frac{M}{\mu}\right) + 12\log^2\frac{M}{\mu} - 8\log\frac{M}{\mu} + \frac{1}{4}\left(22 + \pi^2\right) \right] \Bigg\}\, . \end{aligned} \tag{29}$$

We give the result of the mixed terms in Appendix A. There is in addition a contribution from the purely regular local terms. As already stated the sum of all the regular parts satisfies the Ward identities and thus can be absorbed in the LECs of the Lagrangian of fifth order. We thus refrain from giving any pure two-loop regular pieces here as at the order we are working they are irrelevant. The sum of the mixed and the pure infrared terms (+ the regular parts) above leads to the EOMS expression of the two-loop contribution to the Z factor. Adding the various M^4 contributions to g_A discussed so far one gets:

$$\alpha_4 = -\frac{7}{3} g_0 \left(1 - g_0^2\right) + 16 g_0^5\, . \tag{30}$$

This result agrees with the g_0^5 term of Ref. [14]. However, we found a small mistake in that reference. The quantity $\tilde{\alpha}_4$ which takes into account the quark mass expansion of the decay constant was too large by a factor of two, it should read $\tilde{\alpha}_4 = 2\alpha_2$. Taking this into account and the fact that the result there is given in terms of the physical pion mass our results are in agreement. For γ_4 we get

$$\gamma_4 = \gamma_4^{(0)} + \gamma_4^{(1)} g_0 + \gamma_4^{(2)} g_0^2 + \gamma_4^{(3)} g_0^3 + \gamma_4^{(5)} g_0^5 \,, \tag{31}$$

with

$$\begin{aligned}
\gamma_4^{(0)} &= 16\pi^2 F^2 \left(-20d_{16}^r + 8d_{18}^r + 14d_{10}^r + 8d_{11}^r + 3d_{12}^r + d_{13}^r\right) \,,\\
\gamma_4^{(1)} &= -32\pi^2 F^2 \left(d_{14}^r - 2(d_1^r + d_2^r)\right) - 64\pi^2 \left(l_3^r - l_4^r\right) - \frac{389}{36}\\
&\quad - \frac{64\pi^2 F^2}{m}\left(c_2 + c_3 - c_4 - \frac{1}{2m}\right) \,,\\
\gamma_4^{(2)} &= 256\pi^2 F^2 \left(d_{18}^r - 3d_{16}^r\right) \,,\\
\gamma_4^{(3)} &= -128\pi^2 \left(l_3^r - l_4^r\right) + \frac{1}{9}\left(13 - 16\pi^2\right) + \frac{48\pi^2 F^2}{m^2} \,,\\
\gamma_4^{(5)} &= \frac{11}{3} \,.
\end{aligned} \tag{32}$$

And finally one has

$$\beta_4 = \beta_4^{(0)} + \beta_4^{(1)} g_0 + \beta_4^{(2)} g_0^2 + \beta_4^{(3)} g_0^3 + \beta_4^{(5)} g_0^5 \,, \tag{33}$$

with

$$\begin{aligned}
(4\pi F)^4 \beta_4^{(0)} &= -4\pi^2 \left(2d_{10}^r + 4d_{11}^r + 3d_{12}^r + d_{13}^r\right) + C_0^{(0)} \,,\\
(4\pi F)^4 \beta_4^{(1)} &= -8\pi^2 \left(d_{14}^r + 2(d_1^r + d_2^r)\right) - 32\pi^2 l_3^r + \frac{3575}{864} - \frac{\pi^2}{3} + \frac{1}{2}\psi^{(1)}\left(\frac{2}{3}\right) + C_0^{(1)}\\
&\quad + \frac{16\pi^2 F^2}{m}\left(c_2 + 4c_4 + \frac{2}{m}\right) \,,\\
(4\pi F)^4 \beta_4^{(2)} &= -64\pi^2 F^2 \left(3d_{16}^r - d_{18}^r\right) + C_0^{(2)} \,,\\
(4\pi F)^4 \beta_4^{(3)} &= 32\pi^2 \left(-3l_3^r + l_4^r\right) - \frac{\pi^2}{27}\left(61 + 48\log 3\right) - \frac{335}{432} - \frac{1}{6}\psi^{(1)}\left(\frac{2}{3}\right) + C_0^{(3)} + \frac{32\pi^2 F^2}{m^2} \,,\\
(4\pi F)^4 \beta_4^{(5)} &= \frac{41}{36} + \frac{7}{3}\pi^2 + C_0^{(5)} \,,
\end{aligned} \tag{34}$$

where $\psi^{(1)}(2/3) = 3.06388$ is the first derivative of the digamma function at 2/3. Note that the $\beta_4^{(i)}$ also have contributions from the d_i^ϵ and l_i^ϵ terms in Eqs. (18) and (20), respectively. These can be absorbed in the $C_0^{(i)}$. In the EOMS scheme the mixed terms do not contribute to $\alpha_4^{(i)}$. This has to be the case as the leading non-analytic terms have to be the same in all renormalization schemes. This is in principle not the case for $\gamma_4^{(i)}$ as this coefficient is renormalization scheme-dependent due to the different treatment of one-loop diagrams in different renormalization schemes. It turns out that in our case the mixed terms do not contribute to $\gamma_4^{(i)}$. Thus the only difference between EOMS and IR at that order are terms contributing to β_4. These will be hidden in the $C_0^{(i)}$.

Let us now discuss the convergence of the series and the dependence of g_A on the pion mass which is relevant for the lattice. We will not perform fits to lattice data here, but rather use typical values for the pertinent LECs from various analyses of elastic and inelastic pion-nucleon scattering in the EOMS scheme to get an idea about the size of the leading two-loop corrections. A more detailed discussion including also an uncertainty analysis will be given in Ref. [20]. To be concrete, we use $F_\pi = 0.927$ GeV and $M_\pi = 0.139$ GeV, and the nucleon mass in the chiral limit is taken as $m = 0.87$ GeV [35]. Further, we set the renormalization scale to $\mu = m$ (which leads to $\log(m/\mu) = 0$, a quantity which appears in the mixed terms and in the regular ones in principle) and take the values of the LECs at that scale. The LECs in the mesonic sector are rather well known, one has $l_3(m) = 1.4 \cdot 10^{-3}$ and $l_4(m) = 3.7 \cdot 10^{-3}$. From the values of l_3 and l_4 one can determine F and M. In the baryon sector the LECs are less known. From an analysis of elastic and inelastic pion-nucleon scattering [36] we take set 1 (which is based on the standard power counting $m_N \sim \Lambda_\chi$) $c_2 = 3.51$ GeV^{-1}, $c_3 = -6.63$ GeV^{-1}, $c_4 = 4.01$ GeV^{-1}, $\bar{d}_1 + \bar{d}_2 = 4.37$ GeV^{-2}, $\bar{d}_{10} = -0.8$ GeV^{-2}, $\bar{d}_{11} = -15.6$ GeV^{-2}, $\bar{d}_{12} = 5.9$ GeV^{-2}, $\bar{d}_{13} = 13.6$ GeV^{-2}, $\bar{d}_{14} = -7.43$ GeV^{-2}, and $\bar{d}_{16} = 0.4$ GeV^{-2}, and as set 2 (which is based on the power counting used in nucleon-nucleon scattering $m_N \sim \Lambda_\chi^2/M_\pi$), $c_2 = 4.89$ GeV^{-1}, $c_3 = -7.26$ GeV^{-1}, $c_4 = 4.74$ GeV^{-1}, $\bar{d}_1 + \bar{d}_2 = 3.39$ GeV^{-2}, $\bar{d}_{10} = 10.9$ GeV^{-2}, $\bar{d}_{11} = -30.9$ GeV^{-2}, $\bar{d}_{12} = -10.9$ GeV^{-2}, $\bar{d}_{13} = 27.7$ GeV^{-2}, $\bar{d}_{14} = -7.36$ GeV^{-2}, and $\bar{d}_{16} = -3.0$ GeV^{-2}. Note that we only have information on $\bar{d}_{14} - \bar{d}_{15}$ and we have assumed here $\bar{d}_{15} = 0$. Further, the $\bar{d}_i$ are the $d_i^r(\mu)$ defined at $\mu = M_\pi$, see, e.g., Ref. [37]. These central values have been obtained in heavy baryon chiral perturbation theory from a combined fit to the reactions $\pi N \to \pi N$ and $\pi N \to \pi\pi N$. As we have done an expansion in M/m of the IR and EOMS expressions our results should in fact correspond to the one in the heavy baryon approach. Finally, $\bar{d}_{18} = -0.8$ GeV^{-2} can be related to the Goldberger-Treiman discrepancy [37,38]. For the LEC $C_0 \equiv \sum_i C_0^{(i)} g_0^i$ we assume it to be of natural size, typically of the order of $1/\Lambda_\chi^4$ with $\Lambda_\chi = 0.6$ GeV an estimate of the breakdown scale of the chiral expansion (which is a more conservative estimate than given above and was used in Refs. [18,36]). In Fig. 3 (left panel) we show the chiral expansion of g_A at second, third and fourth order for set 1 of the LECs and similarly for set 2 in the right panel of Fig. 3. The upper fourth order curve corresponds to $C_0(m) = 15$ GeV^{-4}, whereas the lower fourth order curve represents the case $C_0(m) = -15$ GeV^{-4}. While the third order correction is large, as the coefficient α_3 in Eq. (1) is proportional to the large factor $2c_4 - c_3$, we see that the fourth order corrections are rather small for pion masses below 300 MeV, even though some of the dimension-three LECs are rather large. Also, we find that $g_0 = 1.0$ for set 1 and $g_0 = 1.3$ for set 2, in order. Furthermore, at the physical pion mass one has for $C_0^{(i)}(m) = 0$

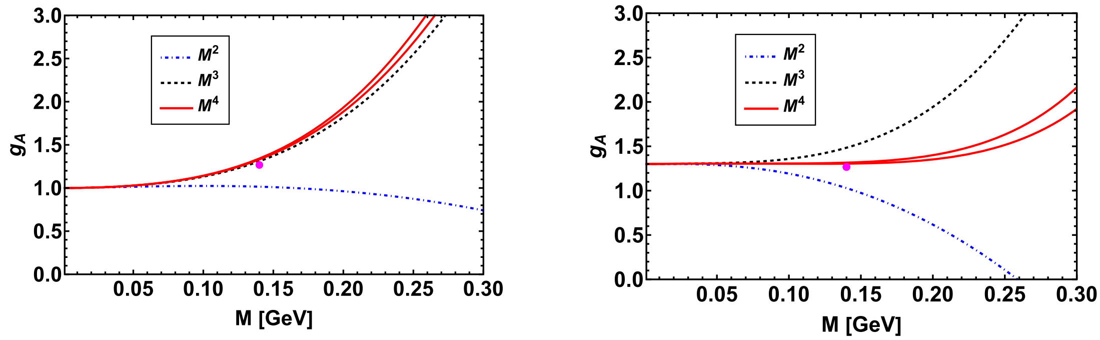

Fig. 3. g_A as a function of M for set 1 (left panel) and set 2 (right panel) of the LECs given in the text. The blue dash-dotted, the black dashed and the red solid lines represent the results up to M^2, M^3 and M^4, respectively. The upper M^4 curve corresponds to $C_0(m) = 15$ GeV^{-4}, whereas the lower M^4 curve represents the case $C_0(m) = -15$ GeV^{-4}. The pink circle denotes the physical value of g_A.

$$\begin{aligned} &\text{set 1}: \Delta^{(2)} = 1.5\%\,, \quad \Delta^{(3)} = 28.8\%\,, \quad \Delta^{(4)} = 2.6\%\,, \\ &\text{set 2}: \Delta^{(2)} = -26.7\%\,, \quad \Delta^{(3)} = 44.5\%\,, \quad \Delta^{(4)} = -17.4\%\,, \end{aligned} \tag{35}$$

which shows the same pattern as discussed above, namely large corrections at order q^3 for both sets of the LECs, but small/moderate ones at leading two-loop order q^4 for set 1 and set 2, respectively. We note that the quantity $\Delta^{(2)}$ is rather sensitive to the actual value of $\bar{d}_{16}$. Furthermore, we point out that in the recent lattice QCD fits in Ref. [9], g_0 comes out in the range $1.26 - 1.30$.

5. Summary and outlook

In this paper, we have calculated and analyzed the leading two-loop corrections to the nucleon axial-vector coupling g_A, that is of fundamental importance in low-energy QCD. We used two covariant versions of baryon chiral perturbation theory, namely we applied the EOMS and the IR renormalization schemes. The pertinent expression for the fourth order corrections $\sim M^4$, denoted as α_4, γ_4 and β_4, as defined in Eq. (1), are explicitly given in Eq. (30), Eq. (31) and Eq. (33), respectively. We have used two sets of the dimension-two and dimension-three LECs from a combined study of the $\pi N \to \pi N$ and $\pi N \to \pi\pi N$ processes in the EOMS scheme and calculated the fourth order corrections as shown in Fig. 3. For set 1 of the LECs, the corrections turned out to be rather small, signaling a good convergence of the chiral expansion of g_A, whereas for set 2 they are larger but still moderate. However, to finally draw conclusions, the M^5 corrections need to be worked out and a more detailed uncertainty analysis has to be performed. Such work is in progress.

Declaration of competing interest

The authors declare that they have no known competing financial interests or personal relationships that could have appeared to influence the work reported in this paper.

Acknowledgements

This work was supported in part by The European Research Council (ERC) under the European Union's Horizon 2020 research and innovation programme (grant agreement No. 101018170). The work of UGM was also supported in part by the CAS President's International Fellowship Initiative (PIFI) (Grant No. 2025PD0022), by the MKW NRW under the funding code NW21-024-A and by the Deutsche Forschungsgemeinschaft (DFG, German Research Foundation) as part of the CRC 1639 NuMeriQS – project no. 511713970. JG acknowledges support by the Georgian Shota Rustaveli National Science Foundation (Grant No. FR-23-856).

Appendix A. Mixed terms in the wave function renormalization factor at two loops

We give the expression of $Z_{(2-\text{loop})}|_{\text{mix}}$, the contribution from the mixed terms $F_2 + F_3$ of the loop functions,

$$\begin{aligned} Z_{(2-\text{loop})}|_{\text{mix}} = \frac{3M^4}{32\pi^4 F^4} g_0 \Bigg\{ & g_0^4 \Bigg(\frac{9\lambda_2}{32} + \lambda_1 \left(-\frac{9}{16}\log\frac{m}{\mu} - \frac{9}{16}\log\frac{M}{\mu} + \frac{71}{192} \right) + \log\frac{m}{\mu}\left(\frac{9}{8}\log\frac{M}{\mu} - \frac{71}{96} \right) \\ & + \frac{9}{16}\log^2\frac{m}{\mu} + \frac{9}{16}\log^2\frac{M}{\mu} - \frac{71}{96}\log\frac{M}{\mu} + \frac{1}{384}\left(113 + 18\pi^2\right) \\ & + g_0^2 \Bigg(-\frac{5\lambda_2}{64} + \lambda_1 \left(\frac{5}{32}\log\frac{m}{\mu} + \frac{5}{32}\log\frac{M}{\mu} - \frac{37}{64} \right) + \log\frac{m}{\mu}\left(\frac{37}{32} - \frac{5}{16}\log\frac{M}{\mu} \right) \\ & - \frac{5}{32}\log^2\frac{m}{\mu} - \frac{5}{32}\log^2\frac{M}{\mu} + \frac{37}{32}\log\frac{M}{\mu} - \frac{5}{384}\left(36 + \pi^2\right) \Bigg) \\ & + \Bigg(-\frac{3\lambda_2}{64} + \lambda_1 \left(\frac{3}{32}\log\frac{m}{\mu} + \frac{3}{32}\log\frac{M}{\mu} - \frac{5}{128} \right) + \log\frac{m}{\mu}\left(\frac{5}{64} - \frac{3}{16}\log\frac{M}{\mu} \right) \\ & - \frac{3}{32}\log^2\frac{m}{\mu} - \frac{3}{32}\log^2\frac{M}{\mu} + \frac{5}{64}\log\frac{M}{\mu} + \frac{1}{256}\left(-33 - 2\pi^2\right) \Bigg\}. \end{aligned} \tag{A.1}$$

One has, see remark after Eq. (29),

$$Z_{(2-\text{loop})}|_{\text{EOMS}} = Z_{(2-\text{loop})}|_{\text{IR}} + Z_{(2-\text{loop})}|_{\text{mix}} + (Z_{(2-\text{loop})}|_{\text{reg}})\,, \tag{A.2}$$

where we put the regular piece in brackets as it is anyway absorbed by the LECs.

Data availability

No data was used for the research described in the article.

References

[1] A. Czarnecki, W.J. Marciano, A. Sirlin, Phys. Rev. Lett. 120 (20) (2018) 202002, arXiv:1802.01804 [hep-ph].
[2] V. Bernard, L. Elouadrhiri, U.-G. Meißner, J. Phys. G 28 (2002) R1–R35, arXiv:hep-ph/0107088 [hep-ph].
[3] J.T. Suhonen, Front. Phys. 5 (2017) 55, arXiv:1712.01565 [nucl-th].
[4] C.C. Chang, A.N. Nicholson, E. Rinaldi, E. Berkowitz, N. Garron, D.A. Brantley, H. Monge-Camacho, C.J. Monahan, C. Bouchard, M.A. Clark, et al., Nature 558 (7708) (2018) 91–94, arXiv:1805.12130 [hep-lat].
[5] Y. Aoki, et al., FLAG Flavour Lattice Averaging Group, arXiv:2411.04268 [hep-lat].
[6] C. Alexandrou, S. Bacchio, J. Finkenrath, C. Iona, G. Koutsou, Y. Li, G. Spanoudes, Phys. Rev. D 111 (5) (2025) 054505, arXiv:2412.01535 [hep-lat].
[7] R.E. Smail, et al., QCDSF/UKQCD/CSSM, Phys. Rev. D 108 (9) (2023) 094511, arXiv:2304.02866 [hep-lat].
[8] Y.C. Jang, et al., Precision Neutron Decay Matrix Elements (PNDME), Phys. Rev. D 109 (1) (2024) 014503, arXiv:2305.11330 [hep-lat].
[9] Z.B. Hall, D.A. Pefkou, A.S. Meyer, T.R. Richardson, R.A. Briceño, M.A. Clark, M. Hoferichter, E. Mereghetti, H. Monge-Camacho, C. Morningstar, et al., arXiv:2503.09891 [hep-lat].
[10] T. Fuchs, J. Gegelia, G. Japaridze, S. Scherer, Phys. Rev. D 68 (2003) 056005, arXiv:hep-ph/0302117 [hep-ph].
[11] T. Becher, H. Leutwyler, Eur. Phys. J. 9 (4) (1999) 643–671, arXiv:hep-ph/9901384 [hep-ph].
[12] V. Bernard, Prog. Part. Nucl. Phys. 60 (2008) 82–160, arXiv:0706.0312 [hep-ph].
[13] U.-G. Meißner, A. Rusetsky, Cambridge University Press, ISBN 978-1-108-68903-8, 2022.
[14] V. Bernard, U.-G. Meißner, Phys. Lett. B 639 (2006) 278–282, arXiv:hep-lat/0605010 [hep-lat].
[15] V. Bernard, N. Kaiser, J. Kambor, U.-G. Meißner, Nucl. Phys. B 388 (1992) 315.
[16] J. Kambor, M. Mojžiš, J. High Energy Phys. 9904 (1999) 031, arXiv:hep-ph/9901235.
[17] M.R. Schindler, T. Fuchs, J. Gegelia, S. Scherer, Phys. Rev. C 75 (2007) 025202, arXiv:nucl-th/0611083 [nucl-th].
[18] D. Siemens, V. Bernard, E. Epelbaum, A. Gasparyan, H. Krebs, U.-G. Meißner, Phys. Rev. C 94 (1) (2016) 014620, arXiv:1602.02640 [nucl-th].
[19] J. Gasser, M.A. Ivanov, E. Lipartia, M. Mojzis, A. Rusetsky, Eur. Phys. J. C 26 (2002) 13–34, arXiv:hep-ph/0206068 [hep-ph].
[20] V. Bernard, J. Gegelia, S. Ghosh, U.-G. Meißner, in preparation.
[21] M.R. Schindler, D. Djukanovic, J. Gegelia, S. Scherer, Nucl. Phys. A 803 (2008) 68–114, arXiv:0707.4296 [hep-ph], Erratum: Nucl. Phys. A 1010 (2021) 122175.
[22] N.D. Conrad, A.M. Gasparyan, E. Epelbaum, EPJ Web Conf. 303 (2024) 02001.
[23] N.D. Conrad, A. Gasparyan, E. Epelbaum, PoS CD2021 (2024) 074.
[24] L.B. Chen, S. Hu, Y. Jia, Z. Mo, arXiv:2406.04124 [hep-ph].
[25] Z.R. Liang, H.X. Chen, F.K. Guo, Z.H. Guo, D.L. Yao, arXiv:2502.19168 [hep-ph].
[26] V. Shtabovenko, R. Mertig, F. Orellana, Comput. Phys. Commun. 256 (2020) 107478, arXiv:2001.04407 [hep-ph].
[27] R. Mertig, R. Scharf, Comput. Phys. Commun. 111 (1998) 265–273, arXiv:hep-ph/9801383 [hep-ph].
[28] T. Huber, D. Maitre, Comput. Phys. Commun. 178 (2008) 755–776, arXiv:0708.2443 [hep-ph].
[29] B. Ananthanarayan, S. Banik, S. Friot, S. Ghosh, Phys. Rev. Lett. 127 (15) (2021) 151601, arXiv:2012.15108 [hep-th].
[30] B. Ananthanarayan, S. Banik, V. Bernard, S. Friot, S. Ghosh, U.-G. Meißner, in preparation.
[31] R. Kaiser, J. High Energy Phys. 09 (2007) 065, arXiv:0707.2277 [hep-ph].
[32] B. Assi, B.A. Kniehl, A.I. Onishchenko, Phys. Rev. D 105 (1) (2022) 016010, arXiv:2110.10662 [hep-ph].
[33] G. Amoros, J. Bijnens, P. Talavera, Nucl. Phys. B 568 (2000) 319–363, arXiv:hep-ph/9907264 [hep-ph].
[34] E. Golowich, J. Kambor, Nucl. Phys. B 447 (1995) 373–404, arXiv:hep-ph/9501318 [hep-ph].
[35] M. Hoferichter, J. Ruiz de Elvira, B. Kubis, U.-G. Meißner, Phys. Rep. 625 (2016) 1–88, arXiv:1510.06039 [hep-ph].
[36] D. Siemens, V. Bernard, E. Epelbaum, A.M. Gasparyan, H. Krebs, U.-G. Meißner, Phys. Rev. C 96 (5) (2017) 055205, arXiv:1704.08988 [nucl-th].
[37] N. Fettes, U.-G. Meißner, S. Steininger, Nucl. Phys. A 640 (1998) 199–234, arXiv:hep-ph/9803266 [hep-ph].
[38] T. Becher, H. Leutwyler, J. High Energy Phys. 06 (2001) 017, arXiv:hep-ph/0103263 [hep-ph].